SAND2008-0778C

Structural and Biophysical Basis of Poxvirus Interaction with Host Cell-Surface Chondroitin Sulfate

Joseph S. Schoeniger, Masood Hadi, Diana Roe, Yooli Light and Marites Ayson
Sandia National Laboratory, Livermore, CA
Brent Segelke and Adam Zemla
Lawrence Livermore National Laboratory, Livermore, CA

INTRODUCTION

Pox viruses cause several disease of significant concern to humans. Variola virus (VARV) causes smallpox, a strictly human disease probably responsible for more human deaths than any other single infectious agent in history. VARV has been eradicated from human populations, but may have been weaponized on a large scale in the former Soviet Union, and remains a potential bioterror threat [1]. Monkeypox occurs sporadically in humans, and is highly pathogenic [2, 3]. Vaccinia virus (VACV), which is of uncertain origin, is used for vaccination against smallpox, and occasionally causes a severe systemic infectious in vaccine recipients or their close contacts [4]. Other endemic pox viruses cause severe disease in animals. To address the potential public health and biodefense threats posed, methods need to be available that can detect malevolent release of poxviruses into the environment, and improved drugs are needed to prevent and treat disease caused by these agents.

The orthopoxviridae are the largest viruses (200x400 nm). They have the largest genome (186 kilobase pairs for VARV) and most genes (~200 open reading frames) of any virus [5]. Nucleotide sequence conservation between species is typically > 90%, but can be as high as 98% [6]. Isolates of VARV are identical to within of 4 amino acids per protein, on average [5]. All orthopoxviruses have a complex replication cycle within the host cell, involving multiple forms, the most abundant of which is the intracellular mature virus (IMV). A potential strategy for developing assays for detection and discrimination of pox viruses is to develop affinity reagents capable of recognizing *unique* protein structural motifs (e.g., epitopes) on the surface of the IMV. It is unclear, however, if the high degree of sequence and structural diversity between species allows this possibility. On the other hand, IMV surface proteins involved in viral attachment and fusion to the host cell are potential drug targets, if it is possible to identify functionally critical and structurally *conserved* binding pocket motifs that can be blocked by ligands.

Four VACV proteins present on the surface of the IMV have been shown to produce neutralizing antibodies when used as exogenous antigens [7]. The sequence diversity of these proteins between different poxviruses is low, however, consisting typically of isolated conservative amino acid substitutions. Since gross-sequence differences cannot reliably be used to generate species *discriminating* antibodies, understanding the structural and biophysical basis of the interaction of these proteins with their cell-surface receptor ligand and other small molecules may assist efforts to improve affinity reagents to detect the smallpox and discriminate it from other pox viruses. Of the four antigenic IMV surface proteins, three bind to host cell-surface glycosaminoglycans (GAGs): 1) D8L binds chondroitin sulfate (CS); 2) H3L and A27L bind heparan sulfate (HS) [8]. VACV mutants lacking D8L have only 6-10% of wild type (wt) infectivity, and H3L- mutants have ~1/6 of wt infectivity [9]. Although glycoreceptors generally are problematic drug targets [10], drugs that blocking the GAG binding sites on these proteins might prove useful in preventing spread of disease, and might be less toxic and more suitable for mass administration than nucleotide analogs such as cidofovir [11].

Previously, we developed tools for identifying unique conserved binding pockets on protein structures [12]. Only one IMV membrane protein (L1R) has been published [13], so we initially attempted to construct homology models for the IMV proteins of interest. Although no suitable templates were found for H3L or A27L, the stretch of 236 C-terminal amino acids of CS binding protein (CSBP) D8L has significant sequence homology to eukaryotic carbonic anhydrase II (CAII) [14]. (The first (removed) 47aa include a transmembrane region with homology to rotavirus proteins.) We identified a positively-charged groove, of the right dimensions for binding CS, and predicted residues potentially involved in CS binding. Using synthesized genes, we expressed D8L (minus its transmembrane anchor), and its VARV homolog F8L, and assayed CS binding affinity and ability to form a stable fold. We also constructed site-specific mutants, and determined effects on CS binding. Subsequently, we determined X-ray structures of D8L and F8L at 1.9Å, and 1.2 Å respectively. We present a preliminary analysis of mutational, biophysical and structural results and discuss their implications for creating assays for discriminating, or drugs for defeating, pox viruses.

METHODS

Modeling: Sequences of CSBP orthologs from poxvirus species were aligned using BLAST or were manually aligned. For structural alignments, orthopox CSBP sequences were aligned with similar structures from the PDB using local-global alignment (LGA), a consensus backbone was chosen, side chains positioned using SCWRL (http://dunbrack.fccc.edu/SCWRL3.php), and residues scored and pockets defined as in Zhou et. al.[12] . Surface electrostatic potential was calculated using DelPhi (http://wiki.c2b2.columbia.edu/honiglab_public/index.php/Software:DelPhi).

Protein Expression and purification: The C-terminal 236 residues of D8L and F8L amino acid sequences from VACV Copenhagen and VARV Bangladesh, respectively, were codon-optimized for *E.coli* and synthesized (Blue Heron Biotechnology, Bothell, WA). Site specific mutants were constructed using Gene Tailor (Invitrogen). The DNA fragments were amplified and cloned into pET-SUMO (Invitrogen, Carlsbad, CA) as described in manufacture's protocol. For expression of truncated D8L and F8l, BL21 Star (DE3) (Invitrogen) cells were transformed with pET-SUMO-D8L/F8L_Trunc and they were grown for 6hrs at 37 °C and induced for 10 hours at 20 °C in Overnight Express™ Instant TB medium (EMD Biosciences, Inc., Madison, WI). Cells were harvested by centrifugation and lysate was obtained by passing through Emulsiflex C-5 (Avestin, Ontario, Canada) 3times followed by centrifugation. The supernatant of the cell lysate was applied to Ni-NTA (Qiagen, Valencia, CA) column equilibrated with the binding buffer. The column was washed with the binding buffer and the proteins bound to the column were eluted with the binding buffer containing 200 mM imidazole. To cleave Sumo tag from D8L/F8L_Trunc, the eluted protein was diluted in 50 mM Tris-HCl (pH 8.0) and cleaved by sumo protease (Lifesensors, Malvern, PA) for overnight at RT. To separate D8L/F8L_Trunc from the cleaved sumo tag, chondroitin sulfate A (Sigma, St Louis, MO) was immobilized on agarose beads pre-activated with cyanogen bromide (Sigma) as described in the manufacture's protocol. The cleaved proteins were buffer-exchanged in 20 mM MOPS with 50 mM NaCl and loaded to the column packed with the chondroitin sulfate agarose beads followed by FPLC using NaCl gradient (0.05-1M).

Structure Determination: Purified D8L/F8L_Trunc were crystallized using hanging drop diffusion following a random screening protocol (Segelke, J. Crystal Growth, 2001). X-ray diffraction data were collected from a single cryo-cooled crystal (Oxford Cryosystems) on Advanced Light Source (ALS) beamline 5.0.2 with an ADSC Quantum 4 CCD x-ray detector. The structure was determined by molecular replacement using human CA II coordinates as the search model.

Biophysical Characterization: Relative binding affinities of wt and mutant protein to CS were determined by order of salt-gradient elution from immobilized CS (above). Melting transitions were determined using differential scanning calorimetry, following the manufacturer's protocol (MicroCal). Binding affinities of CS to immobilized protein were determined using surface plasmon resonance measurements (Biacore 3000).. Briefly, proteins were immobilized onto a CM5 sensor chip and the instrument desorbed using the manufacturers suggested protocols. The binding of CS [in 150mM NaCl or 50mM NaCl in 10mM HEPES pH 7.45] to proteins (R44A, K108A and WT) was determined at 14 different concentrations (0; 0.024414; 0.04888281; 0.0976562; 0.1953125; 0.390625; 0.78125; 1.5625; 3.125; 6.25; 12.5; 25; 50 and 100 µM) in triplicate.

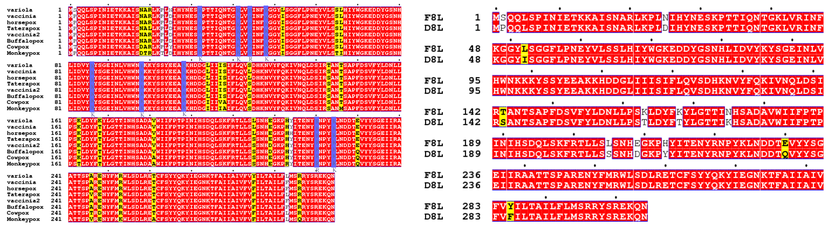

Figure 1. Left: Sequence alignment of CSBP from several orthopox viruses, showing conserved basic residues (blue), conservative mutations (yellow), and non-conservative mutations. Right: Sequence alignment of F8L from VARV Bangladesh with D8L from VACV Copenhagen, which has a N175K basic mutation unique among poxvirus CSBPs.

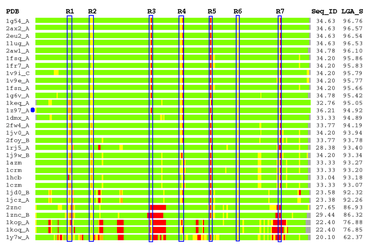

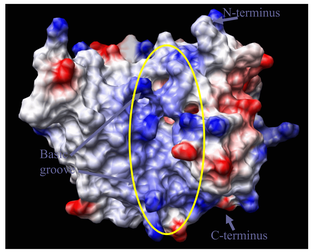

Figure 2. Left: Structural alignment of truncated CSBP consensus backbone model with PDB templates (carbonic anhydrases with and without ligands, mainly). Sequence ID of F8L with human CA II is 34.63%. Most residues align within < 2.0Å (green). Local deviations of > 6Å (red) occur mainly in loops. Right: Electrostatic potential map of consensus homology-based structural model, showing long basic groove.

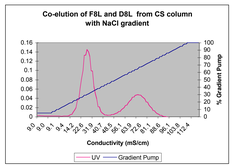

mutants	conductivity (mS/cm) @max A280 1st	2nd	% relative affinity
F8L_WT	59.49		100
D8L_Old(mutation)	20.5	22.5	36.14
K41A	58.36		98.1
R44A	25.51	24.78	42.3
K41A+R44A	18.26	13.46	26.7
K48A	54.99		92.4
R220A	52.55		88.3
K224A	64.87		109.0
R220A+K224A	54.23		91.2
F8L_WT	65.9		100.0
K32A	65.2		98.9
K86A	62.45		94.8
K108A	18.85	18.11	28.0
F8L_WT	60.5		100
K98A	51.9		85.8
N175K	25.8	25.5	42.4
D8L_New	24.14		39.9

relative affinity = ((1st cond. +2nd cond.)/2)/F8L_WT control cond. x100

Figure 3. Left: Characterization of (truncated) D8L (VACV Copenhagen) versus F8L using Chondroitin Sulfate (CS) affinity chromatography (top left) and differential scanning calorimetry. D8L has lower affinity for CS, but is 10 degrees less stable. Middle: Table of relative affinities of different F8L mutants compared to wild type and D8L. The residues that were mutated were selected based on their charge and position relative to the putative binding groove (at Right)

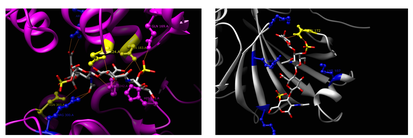

Figure 4. Left: Structure of Chondroitin Sulfate bound to the active site of Chondroitin AB lyase (PDB 1RWG). Right: Preliminary structure of CS docked to F8L consensus structure made with the program AutoDock. Both structures indicate the sulfate is interacting with the asparagine residue, and well as with basic residues.

Binding of CS in 50mM NaCl

Protein	k_a (1/Ms)	k_d (1/s)	K_D (M)
R44A	1.32e3	0.263	199µM
K108A	1.06e3	0.198	186µM
WT	2.6e5	1.87e-3	7.2nM

Binding of CS in 150mM NaCl

Protein	k_a (1/Ms)	k_d (1/s)	K_D
R44A	8.4e2	0.336	400µM
K108A	1.20e3	0.204	171µM
WT	1.39e5	1.86e-3	13.4nM

Figure 5. Results of Surface Plasmon Resonance measurements of CS binding to immobilized proteins at different salt concentrations. Note that the mutants have K_D 3-4 orders of magnitude weaker than the wild type, and that binding is somewhat weaker at the higher salt concentration.

	F8L	D8L
R Factor	20.6	20.0
R Free	23.7	25
B Factor	32.2	28.7
Resolution	1.26 A	1.9 A
Estimated Coordinate Error	0.06	0.17
Data Collection Completeness (theoretical)	99.9%	99.0%
Unique Reflections	44878	15387
Crystal Packing Group	P41	P212121
RMS (deviation from ideal bond distance)	0.013 A	0.033 A
Bond Angle	1.4 degrees	2.4 degrees
Atoms	2011	1905
Residues (Resolved)	233	224
Residues (Unresolved)	#1, 209-210	1-3, 204-213 and last 3
Ramanchandran Plots		
Water	100	59

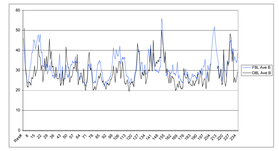

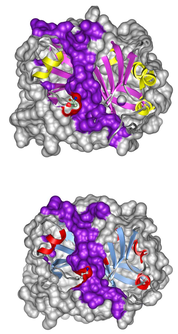

Figure 6. X-ray Crystallography Results for F8L and D8L wild type proteins. Left: Summary of the properties of the structure solutions. Middle Bottom: Different crystal forms observed for the two proteins (Note that the crystal packing differs). Middle Top: Plot of B factors versus residue position, showing that they co-vary. Right: Solvent Accessible surface of F8L (top) and D8L (bottom), explicitly showing next to the groove the N175 side-chain in F8L and K175 in D8L. The RMS deviation from the average CA II template structure is < 0.86Å .

RESULTS AND DISCUSSION

The sequence of CSBPs are highly conserved across poxviruses (Figure 1). Inspection of sequence differences does not allow any simple conclusions to be drawn about their functional role, or potentially useful difference between F8L and D8L. Modeling results indicate that CSBPs should be structurally very similar to CA II proteins, despite moderate levels of sequence identity (Figure 2), and a homology model reveals a positively charged groove that appears well suited for binding an extended anionic ligand such as CS. Surprisingly, we found that the D8L sequence from VACV Copenhagen was not only less stable, but could be more easily salted off a CS affinity column (Figure 3). Although VACV Copenhagen was the first pox virus sequenced, and is often used as a reference genome, close inspection of sequences reveals an asparagine residue at position 175 of all orthopox CSBPs except VACV Copenhagen, which has a lysine. This basic residue might be expected to increase binding to CS, however. To test our homology model, we selected several basic residues for mutation, and found that those near the middle of the groove had a stronger effect on binding that those more peripheral, and that the N175K mutation of F8L has the same affinity for CS, as measured by salt elution (Fig. 3, table). It does not appear that the lessened binding of D8L is related to lower fold stability. Modeling of CS interactions with the binding pocket indicate an important role for N175 similar to that found in CS lyase (Figure 4). To further quantitate the effect of these mutations, we performed SPR measurements that showed the multidentate binding of CS to F8L monolayers to be in the nanomolar range (Figure 5.) To further elucidate the structure and energetics of CS interactions and enable ligand binding studies to proceed on a firm basis, we attempted to crystallize F8L and D8L. We successfully obtained high-quality crystals, and were able to solve structures based on molecular replacement with CA II as a model. The resulting structures are very similar to each other and to CA II, though the less stable D8L formed different, and somewhat lower quality crystals than F8L (Figure 6). B factor analysis does not reveal any disordered regions in D8L relative to F8L . Both structures show the putative binding groove open, though the K175 side chain may protrude into it more than N175.

It appears that CS binding may bind to a contiguous groove in poxvirus CSBPs, unlike the distributed binding sites in many glycoreceptor proteins. Although we are certain from our results that residues in the middle of the groove are important for binding, further studies are needed to provide direct evidence that bound CS is positioned along the length of the groove.

References

(1) Henderson, D. A.; Inglesby, T. V.; Bartlett, J. G.; Ascher, M. S.; Eitzen, E.; Jahrling, P. B.; Hauer, J.; Layton, M.; McDade, J.; Osterholm, M. T.; O'Toole, T.; Parker, G.; Perl, T.; Russell, P. K.; Tonat, K.; Working Grp Civilian, B. *Jama-Journal of the American Medical Association* **1999**, *281*, 2127-2137.
(2) Parker, S.; Nuara, A.; Buller, R. M. L.; Schultz, D. A. *Future Microbiology* **2007**, *2*, 17-34.
(3) Shchelkunov, S. N.; Totmenin, A. V.; Safronov, P. F.; Mikheev, M. V.; Gutorov, V. V.; Ryazankina, O. I.; Petrov, N. A.; Babkin, I. V.; Uvarova, E. A.; Sandakhchiev, L. S.; Sisler, J. R.; Esposito, J. J.; Damon, I. K.; Jahrling, P. B.; Moss, B. *Virology* **2002**, *297*, 172-194.
(4) Bray, M.; Wright, M. E. *Clinical Infectious Diseases* **2003**, *36*, 766-774.
(5) Esposito, J. J.; Sammons, S. A.; Frace, A. M.; Osborne, J. D.; Olsen-Rasmussen, M.; Zhang, M.; Govil, D.; Damon, I. K.; Kline, R.; Laker, M.; Li, Y.; Smith, G. L.; Meyer, H.; LeDuc, J. W.; Wohlhueter, R. M. *Science* **2006**, *313*, 807-812.
(6) Gubser, C.; Smith, G. L. *Journal of General Virology* **2002**, *83*, 855-872.
(7) Ramirez, J. C.; Tapia, E.; Esteban, M. *Journal of General Virology* **2002**, *83*, 1059-1067.
(8) Lin, C. L.; Chung, C. S.; Heine, H. G.; Chang, W. *Journal of Virology* **2000**, *74*, 3353-3365.
(9) Hsiao, J. C.; Chung, C. S.; Chang, W. *Journal of Virology* **1999**, *73*, 8750-8761.
(10) Bovin, N. V.; Tuzikov, A. B.; Chinarev, A. A.; Gambaryan, A. S. *Glycoconjugate Journal* **2004**, *21*, 471-478.
(11) De Clercq, E. *Antiviral Research* **2002**, *55*, 1-13.
(12) Zhou, C. L. E.; Zemla, A. T.; Roe, D.; Young, M.; Lam, M.; Schoeniger, J. S.; Balhorn, R. *Bioinformatics* **2005**, *21*, 3089-3096.
(13) Su, H. P.; Garman, S. C.; Allison, T. J.; Fogg, C.; Moss, B.; Garboczi, D. N. *PNAS* **2005**, *102*, 4240-4245.
(14) Maa, J. S.; Rodriguez, J. F.; Esteban, M. *Journal of Biological Chemistry* **1990**, *265*, 1569-1577.

Acknowledgements

The Authors would like to acknowledge financial support from the Sandia Laboratory Directed Research and Development Program. Sandia National Laboratories is a multi-program laboratory operated by the Sandia Corporation, a Lockheed Martin Company, for the United States Department of Energy Laboratory under contract DE-AC04-94AL85000